Mathematical Modelling and Bending Analysis of Beams

Brajesh Choudhary[1] and Emarti Kumari[2]*

[1,2] Department of Mechanical Engineering, MBM University, Jodhpur-342011, Rajasthan, India
[1]brajesh.14jiec017@jietjodhpur.ac.in, [2]emarti.me@mbm.ac.in

Abstract

In this communication finite element formulation of Euler-Bernoulli beam is done considering Hermites shape functions and illustrated the calculation of stiffness matrix, mass matrix and force vector in detail. Here, considered the various cross-section of beams such as trapezoidal, rectangular, circular, triangular, etc under various loading and boundary conditions to investigate the effect of transverse deflection, shear force and bending moment with change in cross-section of beams by using finite element method based commercial software ANSYS 18.1. Here, present numerical results are validated with analytical results of beams with different cross-sections, loading and boundary conations.

Keywords

Euler-Bernoulli beam, cross-sections, finite element method, Hermites shape functions.

1. Introduction

Beam and Frame Structures: beams are slender members (L >> d for circular cross-section and L >> width or height for the case of rectangular cross-section) that are used for supporting transverse load; axial and shear load in columns. Long horizontal members are used buildings, bridges, helicopter blades and shafts supported in bearings. Whereas frame structures are complex structures made by rigidly connected members used in spacecraft, aircraft, automobile and defense structures.

Luongo *et al*. [1] modeled a one-dimensional beam that will equivalent to two-dimensional space structure such as planar frames and performed static analysis. Copuroglu and Pesman [2] studied the effect of flettner rotors on rolling motion of ships through computational fluid dynamics. Gao *et al*. [3] developed an integrated numerical method using a seakeeping solver and NS solver based on potential flow meter and VOF model; respectively to study the damaged ship behavior. Roy and Kundu [4] reviewed wind induced vibration and its control in power transmission lines. Authors conducted a comparative study based on the performance of various dampers (i.e. VED, TMS, MR and friction damper) to reduce structural vibrations.

Rahmzadeh and Iqbal [5] examined the responses of post-tensioned laminated veneer lumber beam-column subassemblies by employing a three-dimensional finite element method. Recently, static and dynamic characteristics of flat and curved panels have been studied [6-10] considering different loading and boundary conditions. In this paper authors developed mathematical model of beam using Euler-Bernoulli beam theory and compared the numerical results of ANSYS 18.1 with analytical results of Bansal [14].

2. Finite Element Formulation

2.1. Euler-Bernoulli beam element

A schematic representation of Euler-Bernoulli beam with its coordinate un-deformed and deformed configurations is shown in **Figure 1** and **Figure 2**; respectively. Assumptions of Euler-Bernoulli beam is as follows: (a) beam is thin (h/L << 1); and h/L < 0.05 for homogeneous isotropic beam; (b) normal to the neutral axis remains (for thin beam) normal after deformation.
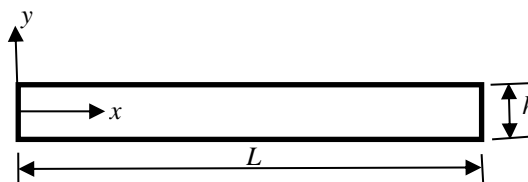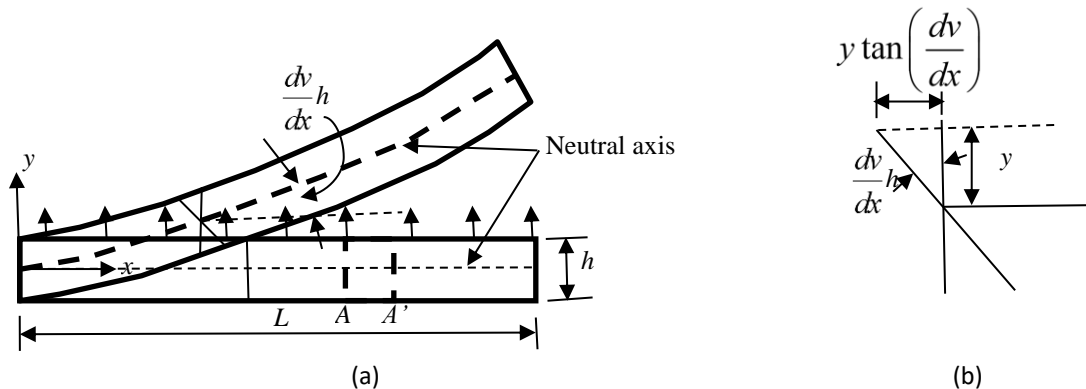

Figure 1.

(a)   (b)

Figure 2. (a) Deformed beam (b) shear strains

Displacement components:

$$u_{(x,y)} = -y\frac{dv}{dx}; \ \ v_{(x,y)} = v_{(x)} \tag{1}$$

Strains:

$$\varepsilon_{xx} = \frac{\partial u}{\partial x} = -y\frac{d^2v}{dx^2} \tag{2}$$

$$\varepsilon_{yy} = \varepsilon_{zz} = -\nu\varepsilon_{xx} \; ; \quad \tau_{xy} = \tau_{yz} = \tau_{zx} = 0 \tag{3}$$

Stress:
$$\sigma_{xx} = E\varepsilon_{xx} = -Ey\frac{d^2v}{dx^2} \tag{4}$$

σ_{yy}, $\sigma_{zz} \cong 0$; approximately zero as its magnitude is very small as compared to σ_{xx}.

Bending moment: systematically expressed in **Figure 3**.

$$M_z = -\int_A y\sigma_{xx}dA \tag{5}$$

By substituting equation (4) into equation (5) we get equation (5) will be written as:
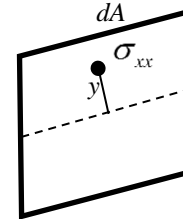
$$M_z = EI_{zz}\frac{d^2v}{dx^2} \tag{6}$$

Figure 3. Bending moment

Systematic representation of forces and moment is shown in **Figure 4;** and Equilibrium equations are written as:
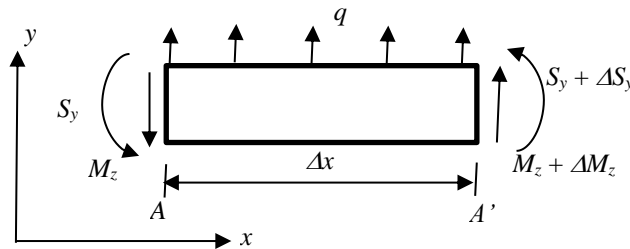

Figure 4. Systematic representation of forces and moment

By resolving forces:

$$\sum F_y = 0 \Rightarrow S_y + \Delta S_y - S_y + q\Delta x = 0 \tag{7a}$$

$$\frac{dS_y}{dx} + q = 0 \tag{7b}$$

$$\sum M_{0z} = 0 \Rightarrow M_z + \Delta M_z - M_z + \left(S_y + \Delta S_y\right)\Delta x + q\Delta x.\frac{\Delta x}{2} = 0 \tag{8}$$

Dividing by Δx both sides and limit $\Delta x \to 0$; get equation (9):

$$\frac{dM_z}{dx} + S_y = 0 \tag{9}$$

Shear force may be expressed as:

$$S_y = -\frac{d}{dx}\left(EI_{zz}\frac{d^2v}{dx^2}\right) \tag{10}$$

By substituting equation (10) into equation (7b), we get:

$$-\frac{d^2}{dx^2}\left(EI_{zz}\frac{d^2v}{dx^2}\right) + q = 0 \tag{11}$$

For finite element formulation, equation (11) is taken weak form then primary variable are: v, $\dfrac{dv}{dx}$ as shown in **Figure 5**.
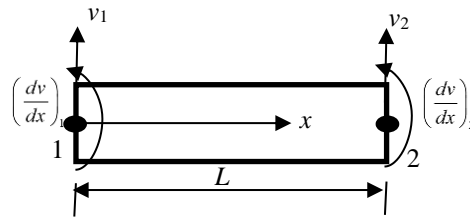
Figure 5. Finite element taken weak form then primary variable

2.2. Total potential energy function

$$I = \frac{1}{2}\int_0^l\int_A E\left(-y\frac{d^2v}{dx^2}\right)^2 dAdx - \int_0^l vqdx - S_{y_2}v_2 - M_{z_2}\left(\frac{dv}{dx}\right)_2 + S_{y_1}v_1 + M_{z1}\left(\frac{dv}{dx}\right)_1 \tag{12}$$

By substituting values of shear force and bending moment at node 1 and 2 such as: $S_{y1} = S_1$, $S_{y2} = S_2$, $M_{z1} = M_1$, $M_{z2} = S_2$,

$$\left(\frac{dv}{dx}\right)_1 = \theta_1 ; \quad \left(\frac{dv}{dx}\right)_2 = \theta_2 .$$

$$I = \frac{1}{2}\int_0^l EI_{zz}\left(\frac{d^2v}{dx^2}\right)^2 dx - \int_0^l vqdx - \sum_i^n S_iv_i - \sum_i^n M_i\theta_i \tag{13}$$

Interpolation polynomial which satisfies the differentiability requirement within element and compatibility conditions as pee order of partial differential governing equations as expressed by Chandrupatla and Belegunda [11]:

$$v = a_0 + a_1x + a_2x^2 + a_3x^3 \tag{14a}$$

At node 1, x = 0 $\quad\quad\quad\quad\quad\quad v_1 = a_0 \quad\quad\quad$ and $\theta_1 = a_1$

and at node 2, x = L $\quad\quad\quad v_2 = v_0 + \theta_1L + a_2L^2 + a_3L^3 ; \quad \theta_2 = \theta_1 + 2a_2L + 3a_3L^2 \tag{14b}$

Thus, $a_0 = v_1 ; \; a_1 = \theta_1 ; \; a_2 = -\frac{3v_1}{L^2} - \frac{2\theta_1}{L} + \frac{3v_2}{L^2} - \frac{\theta_2}{L} ;$ and $a_3 = \frac{2v_1}{L^3} + \frac{\theta_1}{L^2} - \frac{2v_2}{L^3} + \frac{\theta_2}{L^2} \tag{14c}$

Polynomial may be written as:

$$v(x) = \begin{bmatrix} H_1 & H_2 & H_3 & H_4 \end{bmatrix}\begin{Bmatrix} v_1 \\ \theta_1 \\ v_2 \\ \theta_2 \end{Bmatrix} = [H]\{d^e\} \tag{15}$$

Here, H_1, H_2, H_3, H_4 are the Hermits interpolation functions may be described as follows:

$$H_1 = 1 - \frac{3x^2}{L^2} + \frac{2x^3}{L^3} ; \; H_2 = X - \frac{2x^2}{L} + \frac{x^3}{L^2} ; \; H_3 = \frac{3x^2}{L^2} - \frac{2x^3}{L^3} ; \; \text{and} \; H_4 = -\frac{x^2}{L} + \frac{x^3}{L^2} .$$

Integral function may be written as given in equation (16) from equation (13):

$$I = \frac{1}{2}\int_0^l EI_{zz}\left(\frac{d^2v}{dx^2}\right)^T\left(\frac{d^2v}{dx^2}\right)dx - \int_0^l v^T qdx - \begin{Bmatrix} v_1 \\ \theta_1 \\ v_2 \\ \theta_2 \end{Bmatrix}\begin{Bmatrix} -S_1 \\ -M_1 \\ S_2 \\ M_2 \end{Bmatrix} \tag{16}$$

Here, $\frac{d^2v}{dx^2} = \begin{bmatrix} \frac{d^2H_1}{dx^2} & \frac{d^2H_2}{dx^2} & \frac{d^2H_3}{dx^2} & \frac{d^2H_4}{dx^2} \end{bmatrix}\{d^e\} = [B]\{d^e\} \tag{17}$

By substituting the approximation of 'v' in integral function equation (16); we get:

$$I = \frac{1}{2}\{d^e\}^T \left[\int_0^l EI_{zz}[B]^T[B]dx\right]\{d^e\} - \{d^e\}^T \int_0^l [H]^T qdx - \{d^e\}^T \begin{Bmatrix} -S_1 \\ -M_1 \\ S_2 \\ M_2 \end{Bmatrix} \tag{18a}$$

Or $$I = \frac{1}{2}\{d^e\}^T[K^e]\{d^e\} - \{d^e\}^T\{F_{ex}^e\} - \{d^e\}^T\{F_{in}^e\} \tag{18b}$$

For equilibrium of the element: $\delta I = 0$

$$\delta I = \delta\{d^e\}^T[K^e]\{d^e\} - \delta\{d^e\}^T\{F_{ex}^e\} - \delta\{d^e\}^T\{F_{in}^e\} = 0 \tag{19}$$

Here, $[K^e]_{4\times4} = \int_0^L EI_{zz}[B]_{4\times1}^T[B]_{1\times4}\,dx$ and $\{F_{ex}^e\}_{4\times1} = \int_0^L [H]_{4\times1}^T qdx$

Where; $[K^e] = \frac{EI_{zz}}{L^3}\begin{bmatrix} 12 & 6L & -12 & 6L \\ 6L & 4L^2 & -6L & 2L^2 \\ -12 & -6L & 12 & -6L \\ 6L & 2L^2 & -6L & 4L^2 \end{bmatrix}$ and $\{F_{ex}^e\} = q\int_0^L [H]^T dx = q\int_0^L \begin{Bmatrix} H_1 \\ H_2 \\ H_3 \\ H_4 \end{Bmatrix} dx = q\begin{Bmatrix} L/2 \\ L^2/12 \\ L/2 \\ -L^2/12 \end{Bmatrix}$

Here, equation (19) is solved for the bending analysis of beam structures through ANSYS APDL considering linear element.

Dynamic analysis: using equation (14), velocity components are written as described by [12-13]:

$$\dot{v}(x) = [H]\{\dot{d}^e\} \tag{20}$$

Kinetic energy is: $$T = \frac{1}{2}\int_V \dot{v}^2 \rho dV \tag{21}$$

Here, rotational kinetic energy is neglected.

Equation (21) is re-written as equation (22) for the one dimensional problem such as beam/ rod.

$$T = \frac{1}{2}\int_0^L \dot{v}^T\dot{v}\rho A dX \tag{22}$$

By substituting the velocity from equation (20) to equation (22), we get equation (23):

$$T = \frac{1}{2}\int_0^L \{\dot{d}^e\}^T[H]^T[H]\{\dot{d}^e\}\rho A dX \tag{23a}$$

$$T = \frac{1}{2}\{\dot{d}^e\}^T[M^e]\{\dot{d}^e\} \tag{23b}$$

Here, element level mass matrix $[M^e] = \int_0^L [H]^T[H]\rho A dX$

Where, $[M^e] = \frac{\rho A L}{420}\begin{bmatrix} 156 & 22L & 54 & -13L \\ 22L & 4L^2 & 13L & -3L^2 \\ 54 & 13L & 156 & -22L \\ -13L & -3L^2 & -22L & 4L^2 \end{bmatrix}$.

For the dynamic analysis equations of motion is expressed by Hamilton's principle:

$$\int_{t_1}^{t_2}(\delta T - \delta V + \delta W_{NC})dt = 0 \tag{24}$$

Here, δT is a first variation in kinetic energy; δV is a first variation in potential energy of conservative force fields; δW is the virtual work of non-conservative force fields.

Derivative of equation (23b) is expresses as:

$$\delta T = \frac{1}{2}\delta\{\dot{d}^e\}^T[M^e]\{\dot{d}^e\} + \frac{1}{2}\{\dot{d}^e\}^T[M^e]\delta\{\dot{d}^e\} = \delta\{\dot{d}^e\}^T[M^e]\{\dot{d}^e\} \tag{25}$$

Equation (19) may be expressed as equation (26):

$$\delta I = \delta\{d^e\}^T[K^e]\{d^e\} - \delta\{d^e\}^T\{F_{ex}^e\} - \delta\{d^e\}^T\{F_{in}^e\} = \delta V - \delta W_{NC} \tag{26}$$

Therefore, equation (24) might be re-written as equation (27):

$$\int_{t_1}^{t_2}\left[\delta\{\dot{d}_e\}^T[M]_e\{\dot{d}_e\} - \delta\{d_e\}^T[K]_e\{d_e\} + \delta\{d_e\}^T\left[\{F_{ex}^e\} + \{F_{in}^e\}\right]\right]dt = 0 \tag{27}$$

$$\int_{t_1}^{t_2}\delta\{d_e\}^T\left\{[M]_e\{\ddot{d}_e\} + [K]_e\{d_e\} - \{F_{ex}^e\} - \{F_{in}^e\}\right\}dt = 0 \tag{28a}$$

Thus, the governing equation of motion will be written as:

$$[M]_e\{\ddot{d}_e\} + [K]_e\{d_e\} = \{F_{ex}^e\} + \{F_{in}^e\} \tag{28b}$$

Inertial force $\longrightarrow$ Restoring force   External Force

3. Results and Discussion

In this work numerical work has been done using ANSYS software. First some basic analysis of different cross-section beams with point load and UDL has been done on cantilever and simply supported beam. Results of these analysis validated with analytical solutions. Further analysis of trapezoidal cantilever beam has been done using STRUCTURAL module of ANSYS 18.1 workbench. Geometry has been created in design modular and meshing done in ANSYS workbench's meshing tool.

3.1. Bending analysis and validations

Case 1: Square cross-section cantilever (*CF*) beam under point load at the tip of beam as shown in **Figure 6**; made of isotropic material with following material properties:

Young's modulas: E = 200000 MPa; Density: ρ = 7850 kg/m^3;

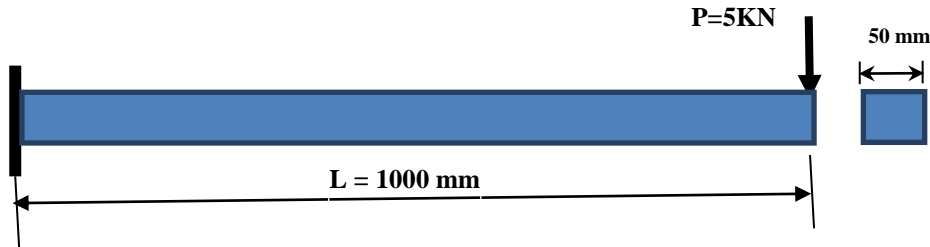Tensile yield strength: σ_t = 250 MPa; Poission's ratio: ν = 0.3

Figure 6. Cantilever beam with point load at tip of beam

An analytically results are calculated as follows [14]:

Tip deflection of beam (for cantilever having point load) $\Delta = \dfrac{PL^3}{3EI}$ = 16 mm

Here, $I = \dfrac{bd^3}{12}$ (for rectangular cross-section) = 520833.33 mm⁴; so, at L = 1000 mm, E = 200 GPa and P = 5000 N.

At $L/2$ i.e. x = 500 mm, from Maxwell's reciprocal theorem.

$$\delta_{L/2} = \delta_{:L/2} + \theta_{L/2} \times \text{(distance between point where load applied and the point where deflection needed)}$$

Deflection at mid-span of beam $\Delta_{L/2}$ = 5 mm; shear stress $\tau = \dfrac{P \times A \times \overline{y}}{I \times b}$ = 0 N/mm²; bending stress $\sigma = \dfrac{M \times y_{max}}{I}$ = 240 N/mm².

Here, shear force P = 5000 N, bending moment M_{max} = 5×10⁶ N-mm, cross-section area A = 2500 mm², distance from natural axis y = 0, width of beam b = 50 mm, area moment of inertia of beam I = 520833.33 mm⁴, y_{max} = 25 mm.

Firstly, validation study of cantilever (*CF*) beam with square cross-section (50 mm×50 mm) having length L = 1000 mm subjected the tip load (P = 5000 N) carried out and compared the numerical results of ANSYS 18.1 Workbench (considering 1D three node quadratic element, with 69 elements and 139 nodes) with analytical results of deflect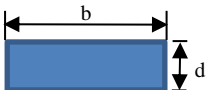ion ($\Delta = \dfrac{PL^3}{3EI}$), shear force and bending moment are as given in **Table 1**. It is found that the numerical results have very good convergence with analytical results with percentage of error 0.18 % for a case of maximum deflection at the tip of beam (x = L); and percentage of error is for the case of shear force and bending moment as given in **Table 1**.

Table 1. Comparison of analytical results with numerical results square cross-section cantilever beam under the tip load (q = 5 KN).

	Method	Max.	Min.	at x = 0	at x = L	at x = L/2
Deflection (mm)	Analytical	16	0	0	16	5
	Present (FEM)	16.03	0	0	16.03	5.01
Shear force (N)	Analytical	5000	5000	5000	5000	5000
	Present (FEM)	5000	5000	5000	5000	5000
Bending moment (N-mm)	Analytical	5×10⁶	0	0	5×10⁶	2.5×10⁶
	Present (FEM)	5×10⁶	1.40×10⁻⁷	1.40×10⁻⁷	5×10⁶	2.5×10⁶

Case 2: Next, Various cross-sections such as rectangular, triangular, circular, and trapezoidal of beam are considered here for the static analysis of beams and presented the area moment of inertia and maximum deflection of these beams in **Table 2**. Moreover, the bending moment and shear force of beams having various cross-sections is evaluated analytically and numerical, and compared these results as given in **Table 3**. Analytically results of beams having different cross-sections: bending moment and shear force will be same for all cross-section:

Table 2. Various cross-sections of beams such as rectangular, triangular, circular, and trapezoidal with its dimension, cross-section area, area moment of inertia and maximum deflection [14].

Shape of Cross-section of beam	Cross-sections	Dimensions with cross-section area	Area moment of inertia	Maximum deflection from natural axis
Rectangular		b = 100 mm d =25 mm	$I = \dfrac{bd^3}{12}$	y_{max} = $d/2$
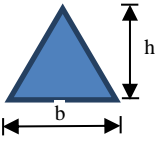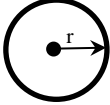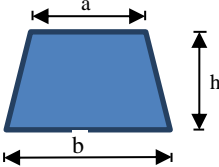
|		A = 2500 mm^2	I = 130208.33 mm^4	
Triangular		b = 100 mm h = 50 mm A = 2500 mm^2	$I = \dfrac{bh^3}{36}$ I = 347222.22 mm^4	y_{max} = $h/3$
Circular		r = 28.21 mm A = 2500 mm^2	$I = \dfrac{\pi d^4}{64}$ I = 497395.92 mm^4	y_{max} = $d/2$
Trapezoidal		a = 40 mm b = 60 mm h = 50 mm A = 2500 mm^2	$I = \dfrac{h^3\left(a^2 + 4ab + b^2\right)}{36(a+b)}$ I = 513888.88 mm^4	$y_{max} = \dfrac{h(2a+b)}{3(a+b)}$ y_{max} = 23.33 mm

Table 3. Validation for same boundary condition and loading condition with different cross-section, keeping the area same for comparison.

| Cross-section Parameters		Square	Rectangular	Triangle	Circle	Trapezium
Area (mm^2)	-	2500	2500	2500	2500	2500
Deflection (mm)	**Analytical**	16	64	24	16.75	16.22
	FEM	16.03	64.03	24.03	16.82	16.242
Bending Stress (N/mm^2)	**Analytical**	240	480	239.90	283.57	226.99
	FEM	240	480	-	284.16	-
Shear stress (N/mm^2)	**Analytical**	0	0	0	0	0
	FEM	0	0	-	0	-

From above results we can say that when area of the all cross- section kept constant then square cross-section performed well and have minimum deflection of 16 mm and trapezium cross-section have lowest bending stress among them, although orientation of the cross-section also affects the results. All results are obtained in ANSYS assuming line body analysis of beam. Results obtained from FEM analysis and analytical are almost same which shows the effectiveness of the FEM analysis. Further validations are done for different loading and boundary condition.

## 3.2. Numerical Results for Cantilever Beam under Point Load

Next, considered the various cross-section of isotropic (v = 0.3) cantilever beam (*CF*) having length (*L* = 1000 mm) such as (a) square cross-section 50 mm × 50 mm; (b) rectangular cross-section 100 mm × 25 mm; (c) triangular cross-section; (d) circular cross-section *r* = 28.21 mm; (e) trapezoidal cross-section 100 mm × 25 mm keeping same cross-section area of these beams i.e. 2500 mm^2. These beams tip deflection are expressed as **Δ**$_{square}$ = 16.031 mm; Δ$_{rectangle}$ = 64.03 mm; Δ$_{triangle}$ = 24.03 mm; Δ$_{circle}$ = 16.82 mm; Δ$_{trapezium}$ = 16.24 mm are presented in **Figure 7 (i)** deflection of the beam at free end and (ii) maximum bending stress.
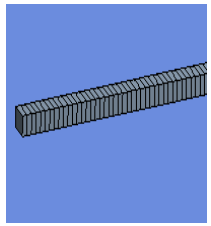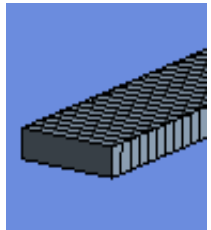
(a)Square cross-section. (50×50)
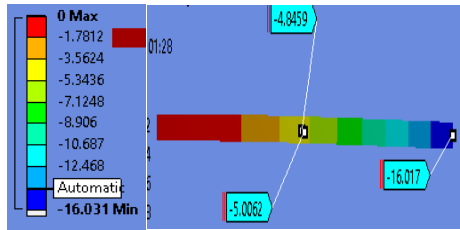
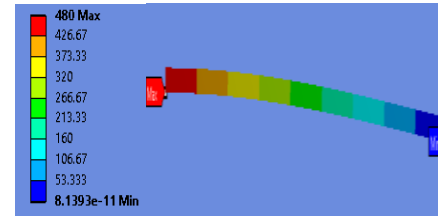(i) Deflection of the beam at L=1000 mm and at mid.(square)(16.031mm)
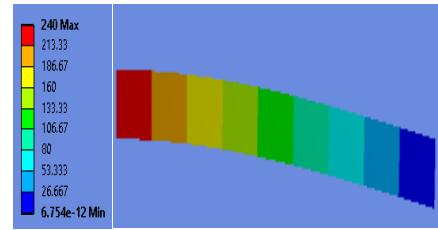
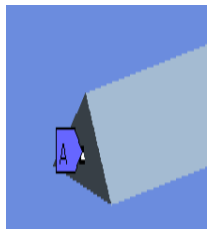(ii) Maximum bending stress of square cross – section beam.(240 N/mm^2)
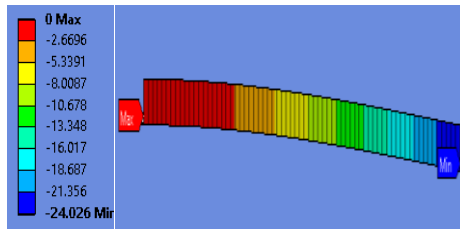

(b)Rectangle cross-section(100×25)
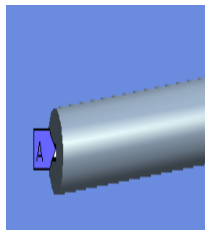
(i) Deflection of the beam at free end

(ii) Maximum bending stress.

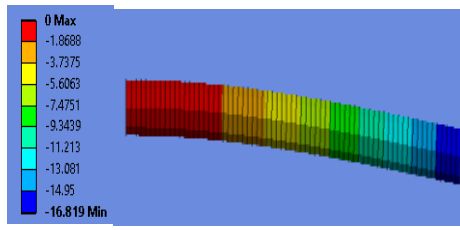(c)Triangular cross-section

(i) Deflection of the beam at free end

(d)Circular cross-section (r = 28.21 mm)

(i) Deflection of the beam at free end
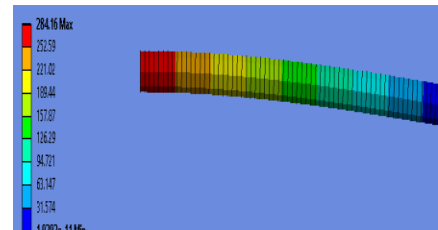
(ii) Maximum bending stress.

(e)Trapezoid cross-section (100×25)

(i) Deflection of the beam at free end
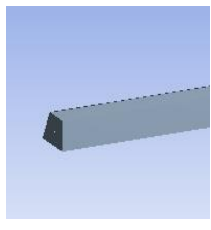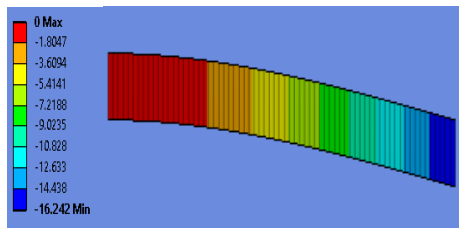
Figure 7. Beams having different cross-sections (a) square, (b) rectangular, (c) triangular, (d) Circular cross-section (r = 28.21) and (e) trapezoid with their (i) deflections of the beams at their tip and (ii) maximum bend-ing stresses.

3.3. Cantilever beam under uniformly distributed load

Now, considering the various cross-section of beams with same material and geometric properties as previous case under uniformly distributed load as shown in **Figure 8**. Here, deflections (mm) and bending stress (N/mm^2) are given in **Table 4** analytically [14] and numerically.

Deflection (for cantilever with UDL) $\quad \Delta = \dfrac{WL^4}{8EI}$
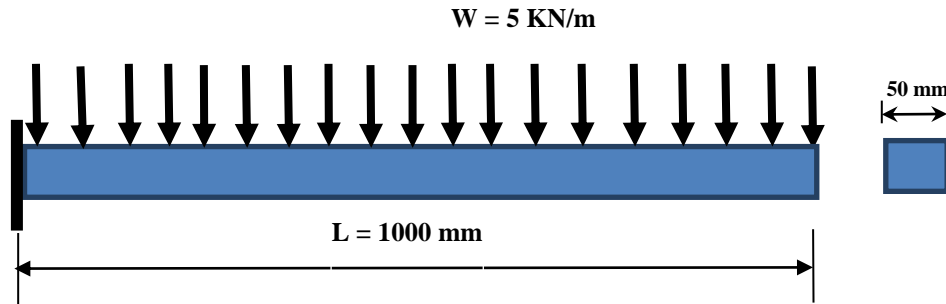
W = 5 KN/m

50 mm

L = 1000 mm

Figure 8. Cantilever beam with UDL

Bending moment and shear force are expressed as follows: Shear force F$_{max}$ = $w \times L$ =5000 N (at L=1000 mm); Bending Moment M$_{max}$ = $w \times L \times (L/2)$ = 2500000 N-mm. Here, analytically: (Bending Moment and shear force will be same for all cross-section) [14].

Table 4. Various cross-section of cantilever (*CF*) beams under uniformly distributed load.

Cross-section Parameters	Results	Square	Rectangle	Triangle	Circle	Trapezium
Area (mm^2)	-	2500	2500	2500	2500	2500
Deflection (mm)	Analytical	6	24	9	6.28	6.08
	FEM	6.015	24.015	9.013	6.31	6.09
Bending Stress (N/mm^2)	Analytical	120	240	119.95	141.78	113.49
	FEM	120	239.99	-	142.08	-

3.4. Simply Supported Beam under Uniformly Distributed Load

Next, considered the various cross-section of simply supported (*SS*) beams (as shown in **Figure 9**) under uniformly distributed load and presented the deflection (mm) and bending stress (N/mm^2) in **Table 5**.
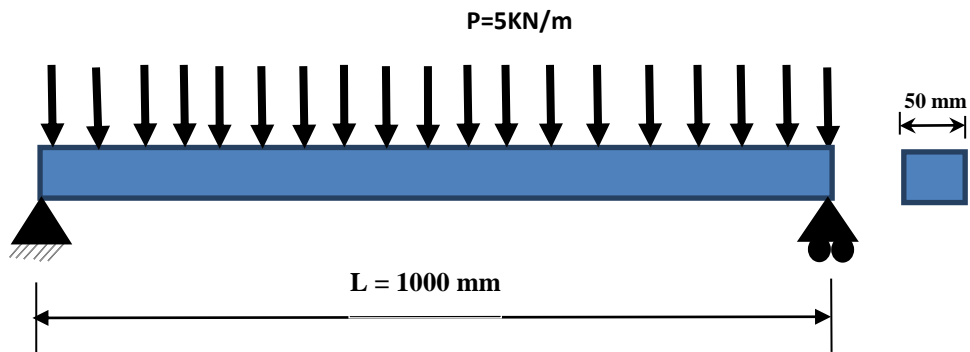
P=5KN/m

50 mm

L = 1000 mm

Figure 9. Simply supported beam subjected uniformly distributed load**.**

Table 5. Various cross-section of simply supported (*SS*) beams under uniformly distributed load.

Cross-section Parameters		Square	Rectangle	Triangle	Circle	Trapezium
Area (mm²)	-	2500	2500	2500	2500	2500
Deflection (mm)	Analytical	0.625	2.5	0.9375	0.6544	0.6334
	FEM	0.628	2.503	0.9407	0.6596	0.6367
Bending Stress (N/mm²)	Analytical	30	60	30	35.447	28.374
	FEM	30.004	60.008	-	35.518	-

4. Conclusion

Here, mathematical modelling of beams is done through finite element approach considering the Euler- Bernoulli beam. Governing equations of motion are derived by using Hamilton's principle. Also, calculated the Hermits shape functions, stiffness matrix, mass matrix and force vector and illustrated here. Thereafter, studied the bending behavior of simply supported and cantilever beams considering five different cross-sections of beams and compared the present numerical results of ANSYS with available analytical results.

References

[1.] Luongo, F. D'Annibale, and M. Ferretti, "Shear and flexural factors for static analysis of homogenized beam models of planar frames," *Eng. Struct.*, vol. 228, no. 111440, p. 111440, 2021. https://doi.org/10.1016/j.engstruct.2020.111440.

[2.] H. I. Copuroglu and E. Pesman, "Analysis of Flettner Rotor ships in beam waves," *Ocean Eng.*, vol. 150, pp. 352–362, 2018. https://doi.org/10.1016/j.oceaneng.2018.01.004.

[3.] Z. Gao, Q. Gao, and D. Vassalos, "Numerical study of damaged ship flooding in beam seas," *Ocean Eng.*, vol. 61, pp. 77–87, 2013. https://doi.org/10.1016/j.oceaneng.2012.12.038.

[4.] S. Roy and C. K. Kundu, "State of the art review of wind induced vibration and its control on transmission towers," *Structures*, vol. 29, pp. 254–264, 2021. https://doi.org/10.1016/j.istruc.2020.11.015.

[5.] A. Rahmzadeh and A. Iqbal, "Numerical modelling and analysis of post-tensioned timber beam-column joint," *Eng. Struct.*, vol. 245, no. 112762, p. 112762, 2021. https://doi.org/10.1016/j.engstruct.2021.112762.

[6.] E. Kumari and S. Lal, "Nonlinear bending analysis of trapezoidal panels under thermo-mechanical load," *Forces Mech.*, vol. 8, p. 100097, 2022. https://doi.org/10.1016/j.finmec.2022.100097.

[7.] E. Kumari, "Dynamic response of composite panels under thermo-mechanical loading," *J. Mech. Sci. Technol.*, vol. 36, no. 8, pp. 3781–3790, 2022. https://doi.org/10.1007/s12206-022-0701-x.

[8.] E. Kumari, "Perspective chapter: Dynamic analysis of high-rise buildings using simplified numerical method," in *Chaos Monitoring in Dynamic Systems - Analysis and Applications*, IntechOpen, 2024. doi: 10.5772/intechopen.108556.

[9.] E. Kumari, "Nonlinear bending analysis of cylindrical panel under thermal load," *International Research Journal on Advanced Science Hub*, vol. 3, no. 7, pp. 145–150, 2021. https://doi.org/10.47392/irjash.2021.191.

[10.] E. Kumari and M. K. Singha, "Nonlinear response of laminated panels under blast load," *Procedia Eng.*, vol. 173, pp. 539–546, 2017. https://doi.org/10.1016/j.proeng.2016.12.086.

[11.] T. Chandrupatla and A. Belegundu, *Introduction to finite elements in engineering*. Cambridge University Press, 2021.

[12.] J. N. Reddy, "An introduction to the finite element method (Vol. 3). *New York: McGraw-Hill*, 2013

[13.] K. J. Bathe, "Finite element procedures". *Klaus-Jurgen Bathe*, 2006.

[14.] R. K. Bansal, "A textbook of strength of materials: (in SI units)" *Laxmi Publications*, 2010.

Authors Profile

Mr. Brajesh Choudhary pursed Bachelor of Technology from Department of Mechanical Engineering, Jodhpur Institute of Engineering and Technology, Rajasthan Technical University, Kota in 2018 and He is currently pursuing Master of Engineering From Deprtment of Mechanical Engineering, MBM University, Jodhpur in the field of Thermal Engineering.

Dr. Emarti Kumari is an Assistant professor in Department of Mechanical Engineering, MBM University Jodhpur. She did her M. Tech. (Design Engineering) and PhD. From Indian Institute of Technology (IIT) Delhi. She is working in the field of computational solid and fluid mechanics (static and dynamic analysis of thin wall-structures), thermal engineering and heat transfer analysis of Laminated Composites, Plates and Shells using Finite Element Methods. She has 12-years teaching experience.